J Mater Sci (2017) 52:2902–2914

Multi-axial forging of Fe_3Al-base intermetallic alloy and its mechanical properties

Radosław Łyszkowski[1,*], Tomasz Czujko[1], and Robert A. Varin[2]

[1] *Faculty of Advanced Technology and Chemistry, Military University of Technology, 2 Kaliskiego Str., 00-908 Warsaw, Poland*
[2] *Department of Mechanical and Mechatronics Engineering, University of Waterloo, Waterloo, ON N2L 3G1, Canada*

Received: 26 September 2016
Accepted: 8 November 2016
Published online: 15 November 2016

ABSTRACT

Tri-axial plane-strain forging was applied to the Fe–28Al–5Cr–0.8Zr–0.04B intermetallic alloy, in order to study its grain refinement and possible improvement in mechanical properties. The forging temperature range was from 20 to 600 °C. The maximum number of forging passes was 67. The deformed microstructure was investigated using electron backscatter diffraction in a scanning electron microscope. At forging temperatures <500 °C, the alloy was very prone to brittle cracking. At the temperature range of 500–600 °C, the overall plasticity of material increased and the cracking tendency was reduced but not completely eliminated. Extensive processes of dynamic recovery/re-crystallization were observed during forging at 600 °C after 10–40 passes. Recrystallized areas with an average grain size of a few micrometers were observed. However, even after severe deformation at 600 °C, resulting from 40 forging passes ($\varepsilon \sim 11.3$), dynamic recrystallization was incomplete and the fraction of low-angle boundaries was still high. The Vickers microhardness substantially increased from 280 HV0.1 to 450 HV0.1 at the center of the sample after both deformations at room temperature as well as after 20–40 cycles at 500–600 °C. However, a further increase of strain for a sample deformed at 600 °C after 67 passes ($\varepsilon \sim 28$) led to quite a significant hardness decrease at the center of the sample. This phenomenon could be associated with the initiation of dynamic recrystallization. None of the samples forged at the 500–600 °C range exhibited any ductility improvement during subsequent tensile testing at room temperature, most likely, owing to the absence of a uniform ultrafine-grained structure developed during forging.

Address correspondence to E-mail: radoslaw.lyszkowski@wat.edu.pl

DOI 10.1007/s10853-016-0584-2

Introduction

The intermetallic Fe–Al alloys are a group of novel materials with interesting structural and functional properties that arise from their internal structure, mainly the tendency to form superstructure [1]. Particularly noteworthy are the intermetallic Fe_3Al-based alloys that could potentially substitute for more expensive superalloys and creep-resistant steels. They are characterized by a combination of interesting functional characteristics such as an excellent resistance to oxidation, sulfidation and carburizing, good resistance to corrosion in sea water, high resistance to wear, erosion, or cavitation, and high strength to weight ratio [2–6]. The Fe_3Al phase, depending on the chemical composition and temperature has either a $D0_3$ or B2 ordered structure, which is derivative of the body-centered cubic BCC or A2 structure. Thus, the Fe_3Al-based alloys meet the von Mises yield criterion, which in turn allows them, at least in theory, to deform plastically [7].

The biggest disadvantage of Fe_3Al alloys is their low ductility and a tendency to brittle fracture at room temperature which significantly impedes plastic working and a wider practical application of these materials [8, 9]. Aside from a question of optimizing the chemical composition in terms of strength and restrictions of environmental fragility, the most important way to improve their ductile behavior is a structural refinement.

It has been reported that the reduction of grain size is the most effective way to improve both ductility and strength of intermetallic alloys, e.g., reducing the grain size of Fe–40Al (at.%) alloy from 200–50 to 10–2 μm increased the yield strength from 300–450 to 450–750 MPa and ductility from 0–4 to 10–20% (for YS = 500 MPa) [10]. This finding has contributed to the development of research on the thermo-mechanical treatments to modify the microstructure of the Fe–Al intermetallic alloys, including a severe plastic deformation (SPD) technique in order to obtain an ultra- or even nanocrystalline structure [11–18].

A severe plastic deformation (SPD) technique owing to its complex state of stress, allows for a high degree of material deformation and refinement of its microstructure [13]. In deformed material, many shear bands appear on a macroscopic scale as a result of mutual intersections that create faults [19]. Structural transformations are the result of accumulated resilient stresses in the material and uneven distribution of energy in its volume. New grains appear in the material which can achieve nanometric size and a large misorientation angle (>15°) if the width of the microbands is also sufficiently small (<500 nm). This mechanism is called the "geometric mechanism of new grains formation" [20–24]. The formation of ultrafine-grained structure is caused by a change in the direction of deformation (e.g., by rotation of sample) resulting in additional intersecting microbands. Finally, the original strongly deformed structure disappears during the structure rebuilding leading to the formation of grains and subgrains of different sizes dependent on conditions of deformation process [20–23]. For this reason, the structure of bulk materials deformed by the SPD methods may be sometimes quite diverse and may consist of volumes having both ultrafine and nanometric grains. The new grains are usually characterized by a bimodal misorientation distribution, exhibiting low and high misorientation angles. With increasing applied strain, there is a gradual increase in the average misorientation angle of newly formed boundaries and the fraction of high-angle grain boundaries [24, 25]. In this paper, multi-axis compression is applied by using the MAXStrain® unit to impose cyclic compression in two mutually orthogonal directions. The principles of this system are described in details in Ref. [26].

Maziasz et al. [27] showed that in the FeAl intermetallic phase alloys, the addition of Mo, Zr, and B/C as well as plastic working led to the grain refinement ($d < 5$ μm), which in turn resulted in a combination of good plasticity, strength, and toughness. Similarly, in the Fe_3Al alloys Valiev and Mukherje [28] managed to produce a nanostructure by high-pressure torsion (HPT) which exhibited a very high tensile strength of 1400–1600 MPa and a ductility of 12%, during tensile test at 300–600 °C. Morris et al. [29] pointed out that the main factor is the degree of deformation. After deformation at $\varepsilon \approx 3.3$ of iron aluminide by rolling, the effects of recovery still dominated resulting in a submicrometric dislocation structure that after annealing at 600 °C became recrystallized into a fine grain structure ($d \approx 10$ μm).

Muszka et al. [30, 31] used multi-axial forging of IF and HSLA steel and achieved a total strain $\varepsilon_c \leq 20$ with an average grain size of 0.3 μm. Observed increase in strength and hardness was explained by beneficial structure changes of the investigated material. Similar results were also noted by Petryk et al. [32] who accomplished at deformation $\varepsilon_c \approx 12$ a

grain refinement of around 0.2 μm by employing a multi-axial forging of IF steel.

Combining dissimilar types of SPD processes increases the degree of deformation and enhances grain refinement. Shi et al. [33] combined equal channel angular pressing (ECAP) followed by forging of cast AZ80 magnesium alloy. Zaharia et al. [21] used multi-directional extrusion (MDE) to working of copper. In both cases, they observed increase in strength compared to the original material with a continued high plasticity.

In this work, in order to develop the ultrafine-grained structure a multi-axial forging of the Fe_3Al-type intermetallic alloy Fe–28Al–5Cr–0.08Zr–0.04B (at.%) at the temperature range of 20–600 °C and varying deformation levels is applied. Moreover, the structure refinement and mechanical properties are also presented. Previous studies [34, 35] showed that this material had a good corrosion resistance, some ductility at room temperature and high strength at elevated temperatures.

Experimental

The Fe-rich iron aluminide alloy with the composition Fe–28Al–5Cr–0.08Zr–0.04B (at.%), further referred to as "Fe–28Al–5Cr," was prepared by induction melting in an argon atmosphere and cast into a cylindrical steel mold. The obtained ingot of 60 mm diameter and 200 mm length was homogenized at 1100 °C for 10 h and subsequently hot-forged at 1100 °C to a final thickness of 25 mm.

The specimens having dimensions of 10 × 10 × 27 mm were cut by electrical discharge machining (EDM) from the hot-forged bar and subsequently subjected to multi-axis forging which was conducted using the MaxStrain system developed by Dynamic Systems Inc. This method is based on the principle of plane-strain compression, wherein deformation occurs in two axes, while fully restraining the third axis. A sample with a rectangular cross section is compressed by a synchronized pair of anvils. After the first compression, the sample is rotated clockwise by 90°, and following the second compression, rotated anticlockwise to its original position. This cycle may be repeated many times, which results in strain accumulation in the deformed sample and substantial grain refinement. More details about MaxStrain technology can be found in Ref. [31]. In the present work, three-axis plane-strain forging was carried out at room temperature (RT), 200 and 400 °C with the application of 2–10 passes and up to 40 and 67 at 500 and 600 °C. The experiments performed up to 400 and 500 °C above were conducted in air and vacuum, respectively. Throughout the process, the sample was heated resistively, and maintained at a preset temperature by the MaxStrain system. The width of the anvil's contact with the deformed sample was 10 mm. The samples were constrained at the ends during the deformation. Determined by the system and based on the current size of the sample, the average strain in a single pass was about 0.3 and the anvil velocity in the course of deformation was 1 s^{-1}. The time interval between the passes was 4 s.

Figure 1 shows a preparation procedure of tensile and other samples for microstructural examination similarly to a procedure reported in [36]. Due to a small volume of the investigated material, non-standard microtension samples with a gauge length of 17 mm and a cross section of 2.5 × 1.0 mm were cut out along the longest axis of the bar using electro-discharge machining (Fig. 1).

In order to evaluate the development of cracks after the initial hot-forging process, an NDT technique based on X-ray computer tomography (CT)

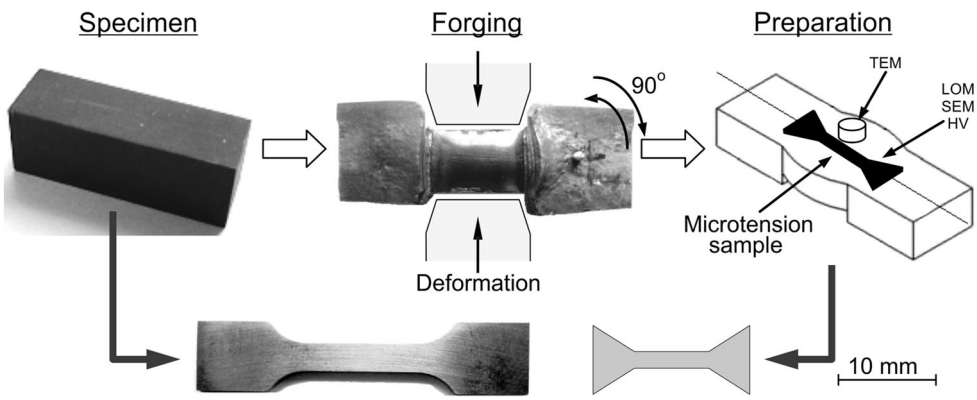

Figure 1 A schematic of multi-axis compression and extraction of tensile samples.

was applied using Nikon/Metris XT H 225ST [37]. Exposures were carried out on bulk samples at X-ray tube voltage of 210 kV and 60 μA intensity, which corresponds to 13.5 W power using a silver target. The results were recorded on a planar array of size 4 megapixel, making 2000 exposures with a single exposure time 1 s. Reconstructed images of samples with an accuracy of 1 pixel, corresponding to the linear dimension of 10 μm.

Furthermore, the deformed specimens were sectioned perpendicularly to the compression direction for microstructural examination. The microstructures of the starting and deformed specimens were characterized by light optical microscopy (LOM) and scanning electron microscopy (SEM) using Philips XL 30 SEM (LaB_6) equipped with a back-scattered electron (BSE) detector mounted in the forward-scattered position underneath the fluorescent screen of the electron backscatter pattern (EBSP) detector. The grain boundary misorientation angles were measured with a ZEISS SUPRA 55VP scanning electron microscope (SEM) using electron back-scattered diffraction (EBSD) with an HKL camera.

The tensile test was performed on a static tensile testing machine Instron 8501 equipped with attachments for non-standard sample tests. Tensile straining was carried out at RT with an initial strain rate of 7×10^{-3} s^{-1}. To determine the deformations occurring during the tensile, test extensometer was used. The fracture surfaces of the tensile-tested samples were examined with a Philips XL30 SEM (LaB_6).

Results

Microstructural evolution upon forging

The samples of the Fe–28Al–5Cr alloy were deformed at the temperature range from 20 to 600 °C and submitted up to 67 passes up to a total strain $\varepsilon \sim 28$. At room temperature, the unit strain was set up at $\varepsilon \sim 0.3$ in relation to the limit of the maximum force which could be applied to the sample. In Fig. 2, the central zone of selected samples after the alternate forging process is shown. Samples deformed at ≤200 °C, having a relatively small deformation degree, exhibited a significant cracking tendency. Resulting deep cracking striations were oriented at an angle of approx. 45° to the axis of the sample which roughly corresponds to the largest shear stress direction in the sample. With increasing temperature, the number of cracks generated from the surface decreased and they completely disappeared at 500 °C. However, the workability still remained very low and only at 600 °C the samples began deforming plastically in a visible way, as evidenced by increasing level of deformation and a pronounced bulging on the sample's surfaces. At such a high temperature, the number of cracks was minimal and their average length was shorter. However, a delamination of the sample occurred at the 67th pass owing to the corresponding accumulation of lattice defects.

Figure 3 shows examples of curves for force versus time and force versus stroke. The occurrence of the forging process was quite similar for all samples. Figure 3a shows that initially the alloy exhibited elastic deformation and after that plastic deformation commenced. The time per pass in the initial stage of the experiment was approx. 0.5 s, while with increasing the number of passes, it was reduced below 0.4 s. As shown in Fig. 3b, for 500 °C the force systematically decreases. However, after exceeding about 10–20 passes (90 s in Fig. 3b), the force becomes nearly saturated. This behavior is owing to the stabilization of deformation and the initiation of dynamic processes such as recovery and/or recrystallization. This behavior was observed at the

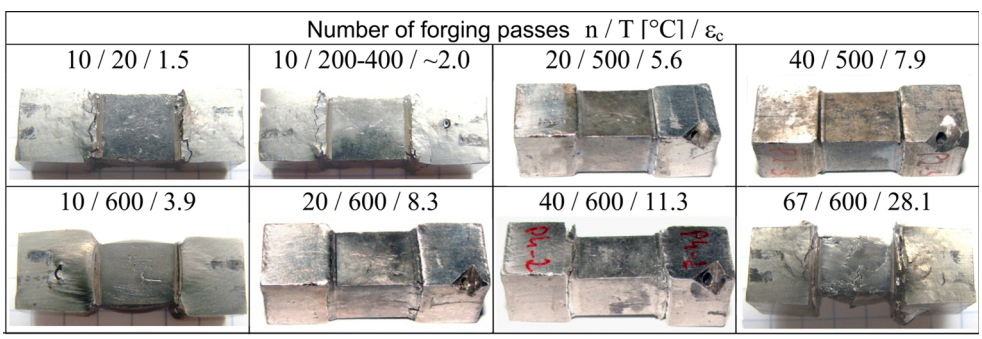

Figure 2 Fe–28Al–5Cr specimens after multi-axis forging using the MaxStrain system at different parameters of deformation. Dimensions of samples: 10 × 10 × 27 mm.

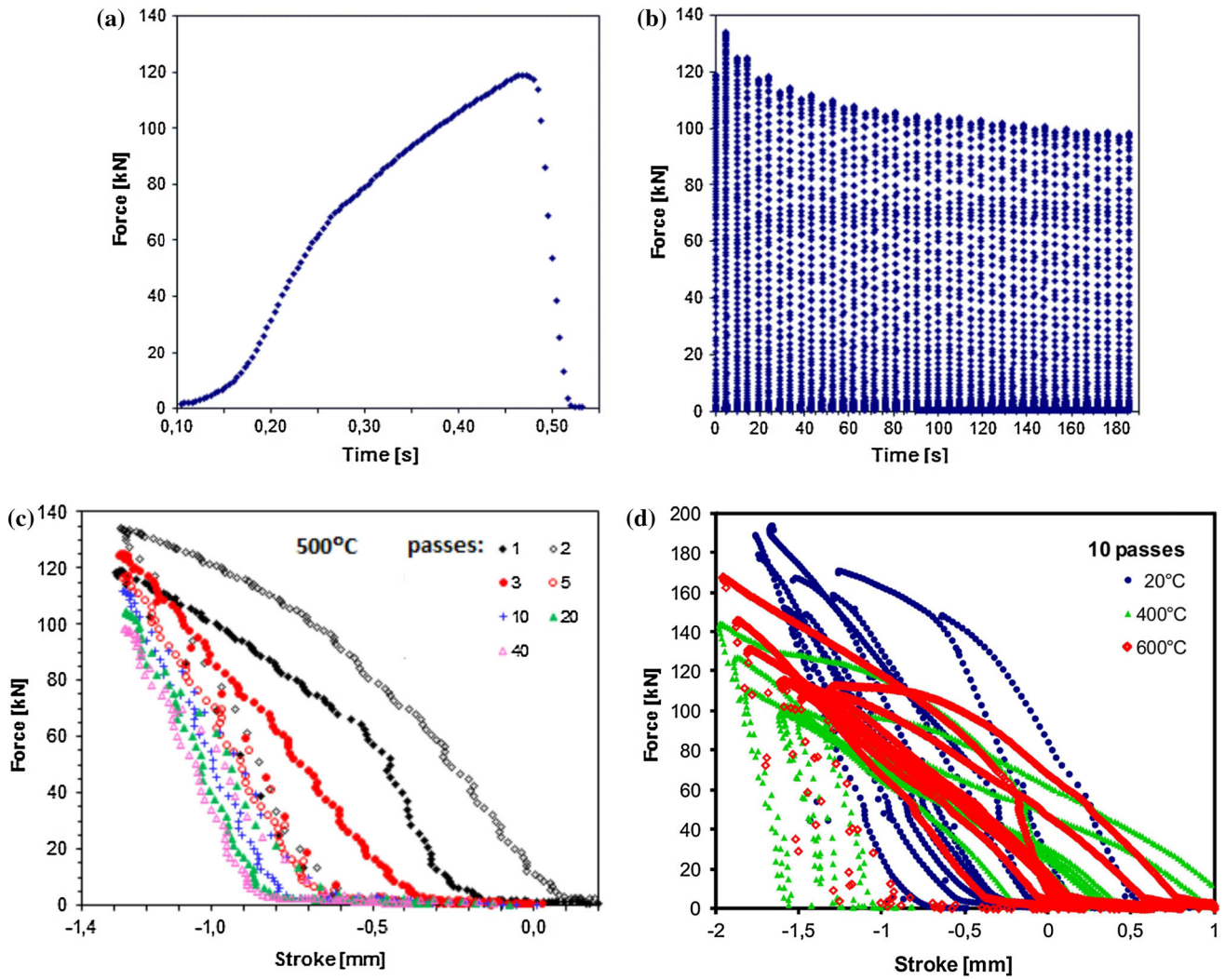

Figure 3 Examples of force versus time plots at 500 °C for first (**a**), following passes (**b**), force versus stroke (**c**), and comparison of 10 first passes at different temperatures (**d**) for multi-axial forging. Following deformation cycles are marked.

temperature range of 500–600 °C which was reflected in the change of the shape of the force/stroke curves which exhibited a reduced force with increasing number (Fig. 3c) and temperature (Fig. 3d) of passes. The increase of stroke within the rise of temperature was also observed, which is associated with increasing plasticity of the material.

An average rate of deformation $\dot{\varepsilon}$ was estimated from the calculated values of the degree of deformation in the individual pass and its duration. For forging at 500–600 °C, it ranged between 0.8 and 1.1 s^{-1}.

The forging process showing a similar behavior was reported by other researchers. Muszka et al. [30] reported two-stage forging process in MaxStrain technology for an IF steel (interstitial-free steel) where initially a decrease of force was observed after which there was a force saturation, similarly to Fig. 3b. The strains achieved at 500 °C are comparable to those reported here. The only difference is the lower level of the applied force in the case of IF steel, due to dissimilar chemical composition to the present intermetallic alloy.

A similar process was reported for the Fe–16Al–5Cr–1Mo–0.1Zr (at.%) alloy in [36]. Due to the increase of aluminum content in the present alloy (28 at.% Al), the deformation of it requires a greater force than that for technical iron alloys investigated in [11] but approx. 10% lower than presented in this paper.

The X-ray computer tomography CT of forged samples allows us to analyze the number and size of existing cracks, their location, and character (Fig. 4a,

b). However, due to the size and nature of the resulting cracks, the CT analysis is suitable for the samples forged under conditions of insufficient plasticity where quite extensive brittle fracture in the gripping sections of the sample was observed, like those forged at temperatures below 400 °C (Fig. 4a) as well as for the samples exhibiting very large deformations at temperatures higher than 400 °C (Fig. 4b).

With increasing temperature, the overall plasticity of material increased and the rate of crack formation was reduced, and the cracks could be closed due to plastic deformation such that above 500 °C for $\varepsilon < 6$ and at 600 °C for $\varepsilon < 10$, no cracks were observed in the deformed areas (Fig. 5). However, the presence of some cracks having sizes beyond the detectability threshold cannot be completely excluded.

EBSD images for microstructure of samples deformed after 10 passes at room temperature (RT) are shown in Fig. 6a. Deformation concentrates within the grains (misorientation distribution within the grains is reflected in various colors on the misorientation maps—Fig. 6a) and the low-angle boundaries (LABs) distribution is inhomogenous. There is no evidence of new grains formation. Similar structure was observed after 10 passes at 200 °C.

As the temperature increased to 400 °C (10 cycles), the plasticity of the material also increased. However, it was still insufficient and did not completely prevent the occurrence of brittle fracture. Euler misorientation maps of grain boundaries in the sample (EBSD) indicate the beginning of the nucleation of new grains in the volume of primary grains. Uneven

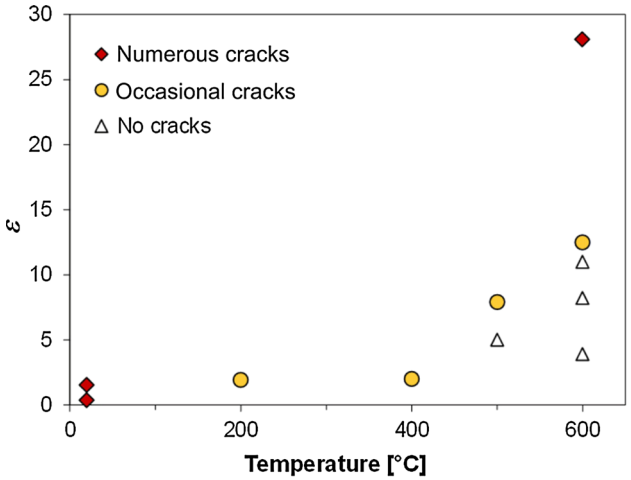

Figure 5 Number of cracks versus strain for the Fe–28Al–5Cr alloy after MaxStrain deformation.

and undulating character of GBs indicates initiation of dynamic recrystallization (Fig. 6b).

A further increase of deformation temperature increased workability of material, which allowed a greater degree of deformation by increasing the number of deformation passes. Thus, a sample deformed after 40 passes at 500 °C, achieved $\varepsilon \approx 7.9$. Its structure was strongly deformed and inhomogenous. New fine grains, with a size about 10 μm, were observed. However, the structure of the entire sample was not recrystallized completely due to still too small a degree of overall deformation and varied greatly in grain size, similarly to the microstructure depicted in Fig. 6b.

Figure 6c shows that the microstructure of a sample deformed after 10 passes at 600 °C exhibits a high

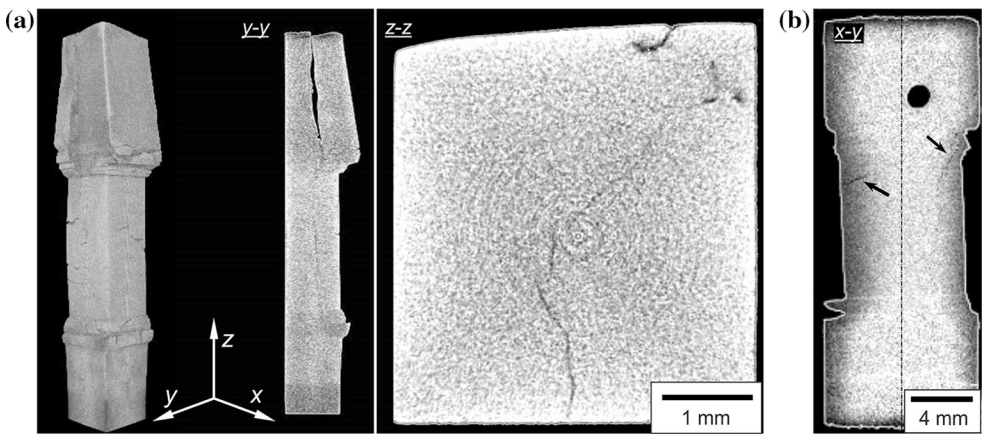

Figure 4 Results of micro-tomography for the Fe–28Al–5Cr alloy: cross-section analysis of ¼ with cracks marked by the *arrows* (description in the text).

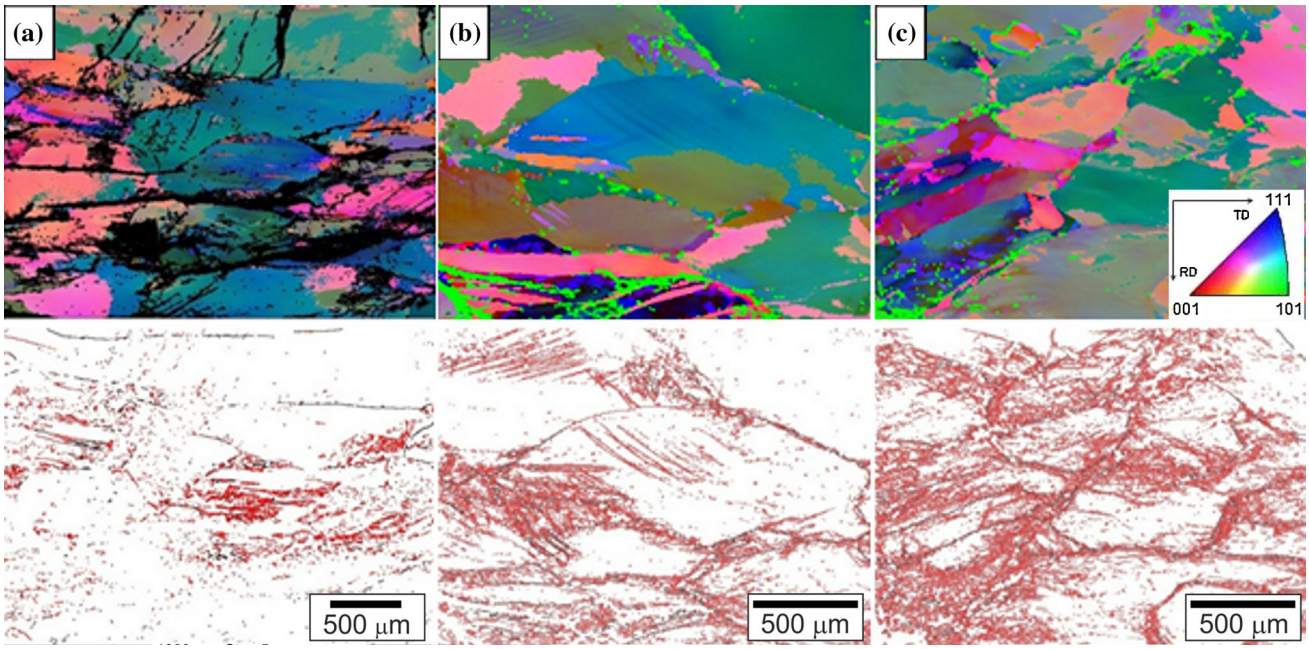

Figure 6 Distribution of low- and high-angle boundaries: **a** 10 passes at RT ($\varepsilon = 1.53$), **b** ×10/400 °C ($\varepsilon = 2.0$), and **c** ×10/600 °C ($\varepsilon = 3.43$). Pictures in the *upper row* Euler misorientation maps and in the *lower row* grain boundaries maps. *Black lines* high-angle boundaries (HABs) (also primary grains), *red lines* low-angle boundaries (LABs) (<2°).

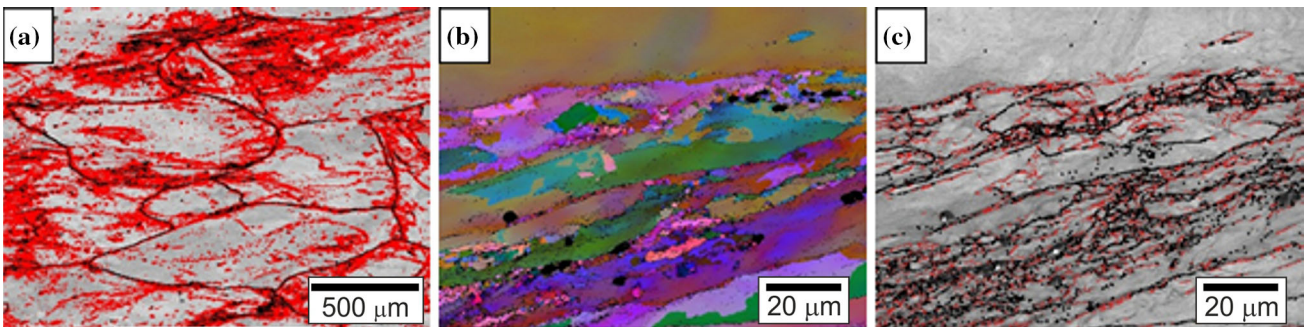

Figure 7 Grain misorientation maps for **a** ×20 and **b**, **c** ×40/600 °C sample (description in the text).

density of low-angle grain boundaries (LABs) homogeneously distributed in the entire volume which promotes the formation of subgrains. Despite a similar deformation strain, the sample after 20 passes at 600 °C ($\varepsilon = 8.3$) (Fig. 7a) seems to be less deformed than the sample after 40 passes at 500 °C ($\varepsilon = 7.9$). The structure observed in Fig. 7a shows a considerable inhomogeneity. Apart from the areas with a high density of LABs, there occur clearly recrystallized areas with low dislocation densities. Initiation of the dynamic recrystallization process usually begins on the primary GBs (Fig. 7a).

The continuation of forging at 600 °C to 40 passes led to a further increase in the degree of deformation ($\varepsilon = 11.3$) (Fig. 7b, c). Dynamic recrystallization processes were much enhanced. There was a significant decrease in the number of LABs (outlined by red lines in Fig. 7c) with simultaneously increasing number of high-angle boundaries (HABs) (outlined by black lines). However, the presence of a large number of deformed grains indicates that dynamic recrystallization is still incomplete.

Fundamental changes in the microstructure are visible in the sample deformed after 67 passes at 600 °C with the accumulated strain reaching $\varepsilon \sim 28.1$ (Fig. 8a–c). The extremely defected structure with a large number of LABs is clearly visible (Fig. 8a). There are areas with a grain size of a few micrometers

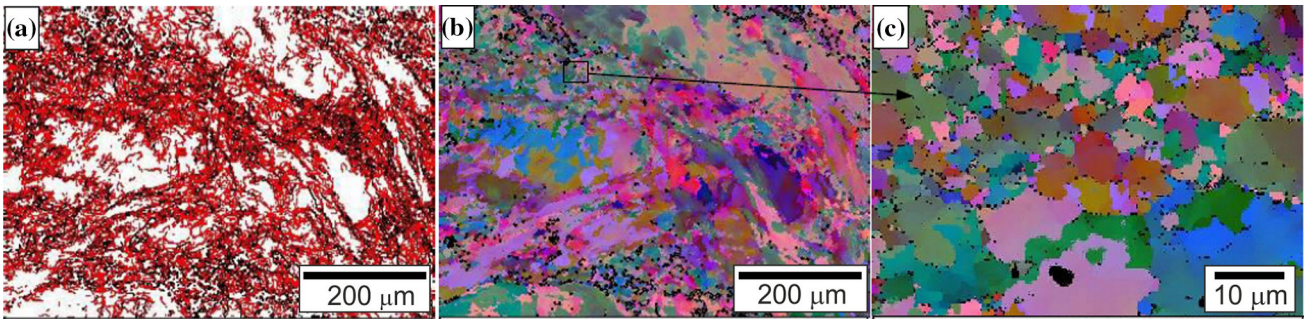

Figure 8 Maps of misorientation grains for ×67/600 °C sample ($\varepsilon = 28.1$—description in the text).

resulting from the occurrence of dynamic recrystallization (Fig. 8b, c). The high density of both LABs and HABs and the areas with high and low degree of mutual misorientation are observed (Fig. 8c-enlarged).

The described changes are in a good agreement with the results reported in [22], where the authors using multi-directional compression (alternately in the x, y, and z directions) of technically pure copper, obtained an overall deformation $\varepsilon = 18$ at the temperature range −78 to 200 °C. Strengthening of material was increasing rapidly but its rate of strengthening in subsequent cycles decreased, reaching the state of plastic flow corresponding to dynamic recrystallization. At an early stage of deformation, above a certain critical stress, numerous shear bands were formed. With the increase of deformation, the number of cells and their misorientation angle increased until they eventually transformed into HABs. Changing the direction of deformation (the x, y, and z directions) accelerated the microstructural evolution through the fragmentation of primary grain boundaries and the rotation of small grain areas and consequently the creation of new fine grains at high strains.

Mechanical properties

In order to evaluate the heterogeneity of deformation, microhardness measurements were carried out according to the scheme shown in Fig. 9. The heterogeneity of deformation is described by the normalized microhardness ratio, *HV01x*/*HV01c*, where *HV01c* is the microhardness in the center of the sample in the initial state, and *HV01x* is the microhardness of the sample at the distance *x* from the center, measured along its longitudinal axis, as shown in the inset in Fig. 9.

Undeformed material has a hardness about 280 HV0.1. A considerable tendency to strain hardening causes visible hardness increase to ~420 HV0.1 in the center of the sample even after 2 passes of deformation at room temperature. As the distance from the center of the sample increases, a slight decrease in the degree of strengthening is observed. At a distance of 4–5 mm from the center, a sharp decrease of hardness is noticed which reaches the value close to the microhardness of undeformed material (Fig. 9). Periodicity of stress changes during forging as well as the increase in temperature causes stress relaxation and a slight decrease in hardness. The accompanying increase in the degree of deformation (number of passes) results in an increase of hardness, which is most visible for the sample deformed at 600 °C after 40 passes ($\varepsilon \sim 11.3$; Fig. 2) (open red triangles in Fig. 9). However, a further increase of strain for a sample deformed at 600 °C after 67 passes ($\varepsilon \sim 28$) leads to quite a significant hardness decrease in the central zone (red squares in Fig. 9). This phenomenon might be associated with the initiation of dynamic recrystallization (Fig. 8). The observed tendency of microhardness distribution has also been described by other researchers who employed a severe plastic deformation (SPD) technique [12, 13].

Since the Fe–Al intermetallic alloys are characterized by substantial brittleness, their fracture and tensile strength are nearly equal and those alloys do not exhibit a visible yielding. Thus, using a static tension test, the basic mechanical properties of the present alloy were evaluated. In the undeformed state, the value of yield strength is 404 MPa, tensile strength 424 MPa, and a total elongation is ~0.5% (Fig. 10a; a green curve). The character of the tensile stress/strain curves for samples deformed at temperatures <500 °C, regardless of the degree of

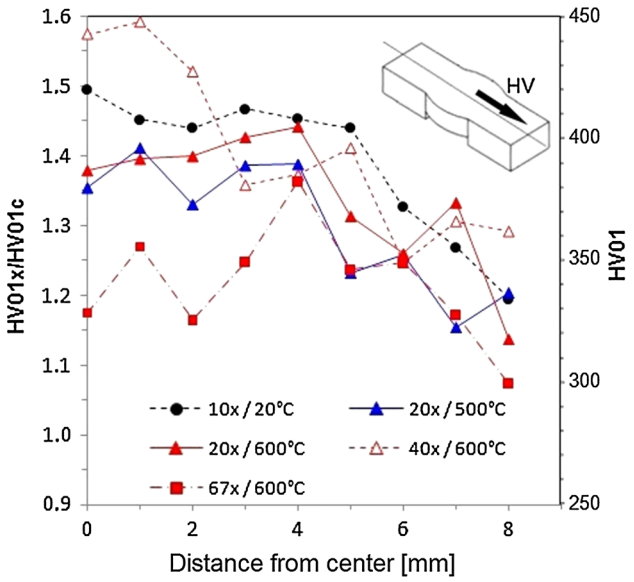

Figure 9 Microhardness distributions in samples after MaxStrain deformation. HV_c—microhardness in the center of sample in initial states, HV_x—the current microhardness value at the distance x from the center in the longitudinal direction.

deformation after forging, indicates that their fracture stress is lower than the yield strength of the undeformed sample (Fig. 10a; a blue curve). This is owing to the occurrence of microcracks in the samples after forging or their strengthening with limited ductility. Similar results were obtained for samples deformed at 600 °C and $\varepsilon < 8$. Furthermore, the increase of strain to $\varepsilon \sim 12$ (40 passes) led to an increase of fracture strength to 424 MPa (Fig. 10a; red line). Unfortunately, plasticity was still insufficient and the sample fractured in a brittle mode at this level of stress.

In order to determine the mechanism of fracture, selected samples after tensile test were investigated using a scanning electron microscope (SEM). These studies show that for samples tested at $T \leq 600$ °C where $\varepsilon < 8$, the material fractures in a brittle cleavage manner. Figure 10b and c shows numerous ledges between parallel terraces, forming probably on the {100} planes and characteristic for this type cracking "river patterns." It is a typical structure of brittle materials such as the alloys based on the intermetallic Fe_3Al phase. In the case of the sample deformed after 40 passes ($T = 600$ °C, $\varepsilon \approx 12$), a general nature of cracking is similar to the previous samples (Fig. 10d). However, the micro-areas indicating the occurrence of plastic deformation with typical "ductile dimples" are also observed (Fig. 10e).

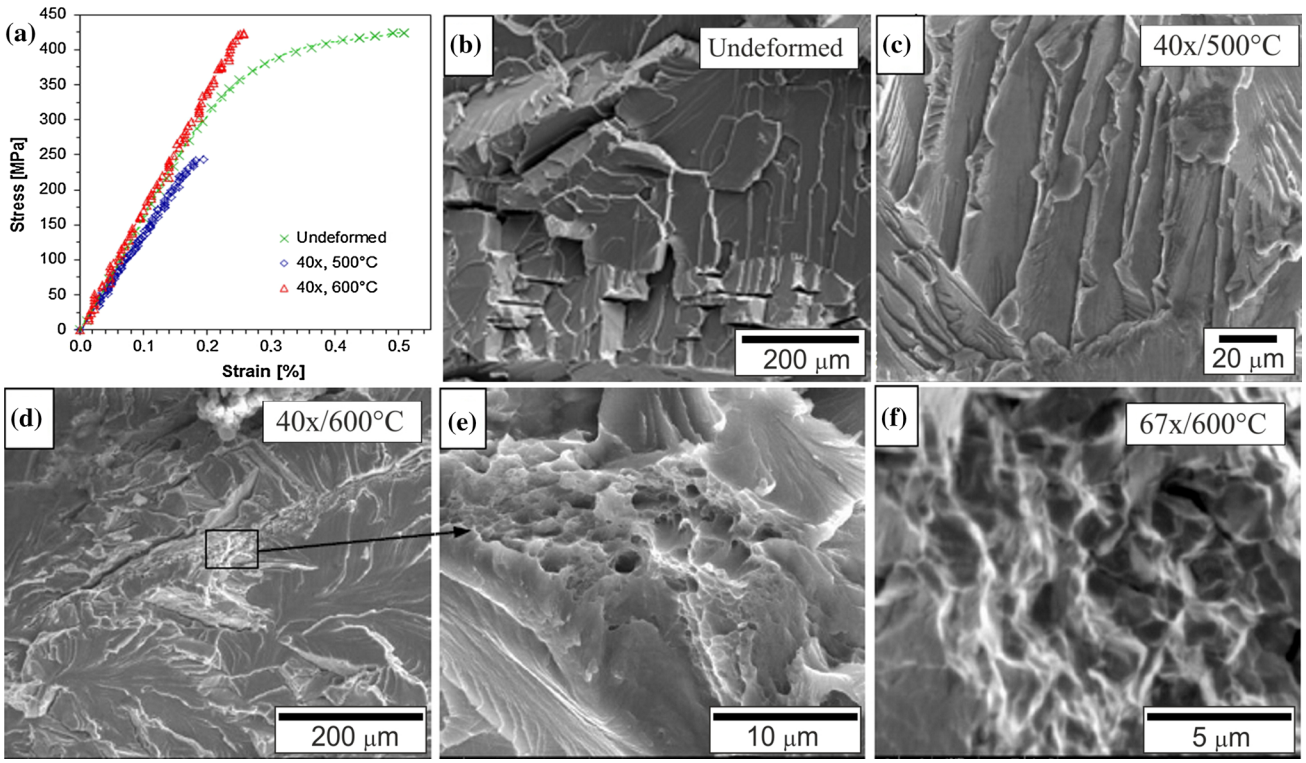

Figure 10 Strain–stress curves and fracture modes of the Fe–28Al–Cr alloy after tensile test at room temperature.

The diameter of dimples is approx. 2–3 μm, which roughly corresponds to the grain size in these microregions (Fig. 7b). Their appearance suggests that the new, dynamically recrystallized grains exhibit a ductile fracture mode, as was the case in Fig. 10f.

Discussion

Morris et al. [29] investigated the rolling process of the Fe_3Al-based intermetallic alloy with similar composition to our material. They showed that for the formation of submicrometric structure it is necessary to create strain with $\varepsilon > 4$, since the lower level of strain causes only accumulation of dislocations with the creation of cellular substructure. This is accompanied by a gradual increase of boundary misorientation and a volume fraction of HABs. However, simultaneous or subsequent recovery and recrystallization are necessary for structure rebuilding to the form of stable sub- or nanocrystalline material. They also indicated that the grains with the orientation close to [113]–[111] recovered and formed a cellular structure much faster than the grains with the orientation [001]. Similar results were also obtained for the alloy based on the Ni_3Al intermetallic phase [38–40].

In the context of the present work, it is important to point out that Sitdikov et al. [41] investigated the behavior of Al 7475 alloy subjected to a multi-directional forging and they described the model of the structure rebuilding during the SPD process. As a result of material deformation, the classical dislocation substructure of nucleating shear microbands was formed. With an increase of strain, an increase of their volume fraction was observed and the grid of intersecting microbands inside the grain was created. As a result of the increasing stress, selected volumes rotated and the formation of new grains occurred. The process of multi-axial forging causing multi-directional shear accelerates the transformation of primary grain microbands into a fine-grained, equiaxed structure. According to Sitdikov et al. [41], the temperature increase intensifies the structure rebuilding process. However, due to the possible occurrence of grain boundary sliding, the strain mechanism adopts a mixed character, combining a microband slip and the nucleation of shear. Thus, the mechanism of plastic deformation gradually changes from the deformation controlled by the movement of dislocations to the deformation associated with the grain boundary sliding.

Tikhonova et al. [20] examined the behavior of AISI 304 steel in the multi-directional pressing at elevated temperatures. At 500 °C (0.45 T_m), large quantities of low-angle boundaries were formed in the deformed material. As a result of accumulated stress and the increased angle of misorientation, these sub-boundaries transformed into a submicron structure, typical for a continuous dynamic recrystallization. Low temperatures prevented boundary migration, regardless of the degree of deformation. At 800 °C (0.6 T_m), a stress decrease and a discontinuous dynamic recrystallization were observed. An increase in the number of new small grains led finally to a development of homogeneous ultrafine-grained structure. Differences in the nature of grain boundaries were associated with different mechanisms of dynamic recrystallization at these temperatures. At 500 °C, a continuous recrystallization with a substructure formation was observed, while at 800 °C a discontinuous recrystallization associated with grain boundary migration occurred.

Based on the above observations and the results of other research [22, 39, 41–43], we can try to generalize the phenomena of plastic deformation occurring during forging of an Fe_3Al-based intermetallic alloy investigated in this work. In the initial stage of deformation, the enormous rise of the dislocation density occurs in the material. Since the Fe_3Al-based alloys belong to the group of materials with a high stacking-fault energy (SFE), dislocations relatively easy organize in the cellular systems, forming the subgrain structure. At low temperatures (in this work $\leq$400 °C), the increase of overall deformation leads only to a greater or lesser increase in the dislocation density (subgrains) and eventually to a possible fracture owing to the microcracks generated in the microstructure. A temperature increase allows thermally activated transformation and reconstruction of the structure to occur. Depending on the temperature, degree of deformation, and chemical composition (the Al content), there is a nucleation of new grains at the primary grain boundaries especially near triple points. Depending on the local conditions, the migration of grain boundaries can occur which can lead to the nucleation of new, very fine grains on the dynamic recrystallization fronts. This process is called necklace recrystallization [43]. However, if the degree of deformation is insufficient like in the

present work, only a few new recrystallized grains are formed in the vicinity of grain boundaries and, in general, the dynamic recrystallization process remains incomplete.

It must be noticed that the Fe_3Al-based alloys are also characterized by a high propensity to structural recovery. It was mentioned earlier that structural recovery can considerably delay the start of recrystallization or even block it owing to an insufficient deformation. At a lower rate of deformation, the influence of structural recovery is more pronounced and recrystallization can only occur at much higher temperatures of deformation. Therefore, the introduction of various deformation paths by the sample rotation between the subsequent cycles of deformation, as it is the case for multi-axial forging, promotes the formation of spatial slip bands of dislocations within the grains which can promote an earlier start of dynamic recrystallization.

Summary and conclusions

The samples of the Fe_3Al-type intermetallic alloy, having a chemical composition (at.%) Fe–28Al–5Cr–0.8Zr–0.04B, were multiaxially forged at the temperature range of 20–600°C with the application up to 67 passes using a MaxStrain system. At forging temperatures <500 °C, the alloy was very prone to brittle cracking, while at the temperature range of 500–600 °C, the overall plasticity of material increased which was accompanied by a reduced cracking tendency. Dynamic recovery/recrystallization occurred during forging at 600 °C after 10–40 passes of deformation resulting in recrystallized volumes exhibiting recrystallized grains with an average size of a few micrometers. However, even after severe deformation after 40 passes at 600 °C (accumulated strain $\varepsilon \sim 11$), dynamic recrystallization was incomplete and the fraction of low-angle boundaries (LABs) was still high. The Vickers microhardness increased to ~420 to 450 HV0.1 at the center of the sample after deformation at room temperature as well as after 20–40 passes at 500–600 °C from its initial value of about 280 HV0.1 for undeformed material. A further strain increase up to $\varepsilon \sim 28$ at 600 °C after 67 passes led to a precipitous hardness decrease at the center of the sample, most likely, owing to the development of dynamic recrystallization. No ductility improvement over the initial undeformed sample was observed for any sample forged at the 500–600 °C range, during tensile testing at room temperature, most likely, owing to the lack of a uniform ultrafine-grained structure developed during forging.

Acknowledgements

The authors thank Prof. A. Fraczkiewicz from the Ecole Nationale Supérieure des Mines de Saint-Étienne, France, for stimulating discussions. The involvement of Ms. Izabela Kunce in the EBSD investigations is acknowledged. This work was supported by the National Science Centre, Poland (Grant No. 2012/05/D/ST8/02710).

References

[1] Sikka VK, Viswanathan S, Mc Kamey CG (1993) Development and commercialization status of Fe_3Al-base intermetallic alloys. In: Darolia R, Lewandowski JJ, Liu CT, Martin PL, Miracle DB, Nathal MV (eds) Structural Intermetallics, vol 483. TMS, Warrendale

[2] Deevi SC, Sikka VK, Liu CT (1996) Nickel and iron aluminides: an overview on properties, processing and applications. Intermetallics 4:357

[3] Judkins RR, Rao US (2000) Fossil energy applications of intermetallic alloys. Intermetallics 8:1347

[4] Matysik P, Jóźwiak S, Czujko T (2015) Characterization of low-symmetry structures from phase equilibrium of Fe–Al system—microstructures and mechanical properties. Materials 8:91

[5] Siemiaszko D, Kowalska B, Jóźwik P, Kwiatkowska M (2015) The effect of oxygen partial pressure on microstructure and properties of Fe40Al alloy sintered under vacuum. Materials 8:1513

[6] Senderowski C (2014) Nanocomposite Fe–Al intermetallic coating obtained by gas detonation spraying of milled self-decomposing powder. J Therm Spray Technol 23:1124

[7] Dieter EG, Kuhn AH, Lee Semiatin S (eds) (2003) Handbook of workability and process design. ASM International, Materials Park
[8] Morris DG, Muñoz-Morris MA (2011) Recent developments toward the application of iron aluminides in fossil fuel technologies. Adv Eng Mater 13:43
[9] Falat L, Schneider A, Sauthoff G, Frommeyer G (2005) Mechanical properties of Fe–Al–M–C (M = Ti, V, Nb, Ta) alloys with strengthening carbides and Laves phase. Intermetallics 13:1256
[10] Morris DG, Morris-Muñoz MA (1999) The influence of microstructure on the ductility of iron aluminides. Intermetallics 7:1121
[11] Valiev RZ (2007) The new trends in fabrication of bulk nanostructured materials by SPD processing. J Mater Sci 42:1483
[12] Langdon TG (2007) The processing of ultrafine-grained materials through the application of severe plastic deformation. J Mater Sci 42:3388
[13] Valiev RZ, Islamgaliew RK, Alexandrov IV (2000) Bulk nanostructured materials from severe plastic deformation. Prog Mater Sci 45:103
[14] Azushima A, Kopp R, Korhonen A, Yang DY, Micari F, Lahoti GD, Groche P, Yanagimoto J, Tsuji N, Rosochowski A, Yanagida A (2008) Severe plastic deformation (SPD) processes for metals. CIRP Ann-Manuf Technol 57:716
[15] Varin RA, Czujko T, Bystrzycki J, Calka A (2002) Cold-work induced phenomena in B2 FeAl intermetallics. Mater Sci Eng 329:213
[16] Jabłońska M, Bednarczyk I, Rodak K, Śmiglewicz A (2016) Study of the structure of intermetallics from Fe–Al system after the hot rolling. Metalurgija 55:67
[17] Bednarczyk I, Jabłońska M (2016) Structural characterization of FeAl28Cr5 alloy deformed in the hot torsion process. Solid State Phenom 246:43
[18] Kratochvíl P, Schindler I (2007) Hot rolling of iron aluminide Fe28.4Al4.1Cr0.02Ce (at%). Intermetallics 15:436
[19] Richert M, Richert J, Zasadziński J, Hawryłkiewicz S, Długopolski J (2003) Effect of large deformations on the microstructure of aluminium alloys. Mater Chem Phys 81:528
[20] Tikhonova M, Kaibyshev R, Fang X, Wang W, Belyakov A (2012) Grain boundary assembler developer in an austenitic stainless steel during large strain warm working. Mater Charact 70:14
[21] Zaharia L, Chelariu R, Comaneci R (2012) Multiple direct extrusion: a new technique in grain refinement. Mater Sci Eng 550:293
[22] Sakai T, Miura M, Yang X (2009) Ultrafine grain formation in face centered cubic materials during severe plastic deformation. Mater Sci Eng 499:2
[23] Sanusi KO, Oliver GJ (2009) Effects of grain size on mechanical properties of nanostructured copper alloy by severe plastic deformation (SPD) process. J Eng Des Technol 7:335
[24] Polkowski W, Jóźwik P, Polański M, Bojar Z (2013) Microstructure and texture evolution of copper processed by differential speed rolling with various speed asymmetry coefficient. Mater Sci Eng 564:289
[25] Polkowski W, Jóźwik P, Łyszkowski R (2016) Effect of hot differential speed rolling on microstructure and mechanical properties of Fe3Al-based intermetallic alloy. Int J Mater Res 107(9):867. doi:10.3139/146.111401
[26] Chen WC, Ferguson DE, Ferguson HS, Mishra RS, Jin Z (2001) Development of ultrafine grained materials using the MAXStrain (R) technology. Mater Sci Forum 357(359):425. doi:10.4028/www.scientific.net/MSF.357-359.425
[27] Maziasz PJ, Alexander DJ, Wright JH (1997) High strength, ductility, and impact toughness at room temperature in hot-extruded FeAl alloys. Intermetallics 5:547
[28] Valiev RZ, Mukherje AK (2001) Nanostructures and unique properties in intermetallics, subjected to severe plastic deformation. Scr Mater 44:1747
[29] Morris DG, Gutierrez-Urrutia I, Morris-Muñoz MA (2008) Evolution of microstructure of an iron aluminide during severe plastic deformation by heavy rolling. J Mater Sci 43:7438
[30] Muszka K, Hodgson PD, Majta J (2006) A physical based modeling approach for the dynamic behavior of ultrafine grained structures. J Mater Process Technol 177:456
[31] Majta J, Muszka K (2007) Mechanical properties of ultra fine-grained HSLA and Ti–IF steel. Mater Sci Eng 464:186
[32] Petryk H, Stupkiewicz S, Kuziak R (2008) Grain refinement and strain hardening in IF steel Turing multi-axis compression: experiment and model ling. J Mater Process Technol 204:255
[33] Shi BQ, Chen RS, Ke W (2012) Effects of forging processing on the texture and tensile properties of ECAEed AZ80 magnesium alloy. Mater Sci Eng 546:323
[34] Łyszkowski R, Bystrzycki J (2007) Influence of temperature and strain rate on the microstructure and flow stress of iron aluminides. Arch Metall Mater 52:347
[35] Łyszkowski R (2015) High-temperature oxidation of Fe_3Al intermetallic alloy prepared by additive manufacturing LENS. Materials 8:1499
[36] Bystrzycki J, Fraczkiewicz A, Łyszkowski R, Mondon M, Pakieła Z (2010) Microstructure and tensile behavior of Fe–16Al-based alloy after severe plastic deformation. Intermetallics 18:1338–1343
[37] http://www.nikonmetrology.com/en_EU/Products/X-ray-and-CT-Inspection. Accessed 01 Aug 2016
[38] Rentenberger C, Waitz T, Karnthaler HP (2007) Formation and structures of bulk nanocrystalline intermetallic alloys

studied by transmission electron microscopy. Mater Sci Eng 462:283

[39] Polkowski W, Jóźwik P, Bojar Z (2015) Differential speed rolling of Ni_3Al based intermetallic alloy—analysis of the deformation process. Mater Lett 139:46

[40] Polkowski W, Jóźwik P, Karczewski K, Bojar Z (2014) Evolution of crystallographic texture and strain in a fine-grained Ni_3Al (Zr, B) intermetallic alloy during cold rolling. Arch Civ Mech Eng 14:550

[41] Sitdikov O, Sakai T, Miura H, Hama C (2009) Temperature effect on fine-grained structure formation in high-strength Al alloy 7475 during hot severe deformation. Mater Sci Eng 516:180

[42] Łyszkowski R, Bystrzycki J (2014) Hot deformation and processing maps of a Fe–Al intermetallic alloy. Mater Charact 96:196

[43] Ponge D, Gottstein G (1998) Necklace formation during dynamic recrystallization: mechanisms and impact on flow behavior. Acta Mater 46:69